CONF-75-190-E

S. Segler 2

Rockefeller University
COO-2232A-23

HIGH ENERGY $pd \to Xd$ DIFFRACTION DISSOCIATION: COMPARISON TO $pp \to Xp$ AND ANALYSIS

USA - USSR Collaboration

at the Internal Gas Jet Target of Fermilab

Cross-sections for the reaction $pp \to Xp$ in the diffraction dissociation region, extracted from the recently reported precise Fermilab data on $pd \to Xd$, are compared with results from Fermilab and ISR. The M_X^2, t, and s dependence are discussed and the first-moment finite mass sum rule is tested.

Submitted to the International Conference on High Energy Physics
Palermo, Italy, June 23-28, 1975

K. Goulianos
Rockefeller University
New York, N.Y. 10021

In two recent publications[1,2] we reported the results of a precise measurement of the inclusive inelastic process

$$p + d \rightarrow X + d \tag{1}$$

in the region $50 < p_{lab} \lesssim 400$ GeV/c, $0.03 < |t| \lesssim 0.12$ (GeV/c)^2, and 1.4 GeV$^2 < M_x^2 \lesssim 0.12\ (m_p \cdot p_{lab})$. This range of M_x^2 includes the resonance region as well as the triple-Regge region[3] (TR region: $M_x^2 >> m_p^2$ and $M_x^2/s \lesssim 0.1$). In this report, we analyze our results using TR phenomenology and we test the first-moment finite mass sum rule[4] (FMSR).

Our analysis is performed on $pp \rightarrow Xp$ cross-sections extracted from our $pd \rightarrow Xd$ data using factorization arguments. By comparing our extracted $pp \rightarrow Xp$ results with existing data we show that factorization holds to a good approximation. In any case, since the reduction to $pp \rightarrow Xp$ cross-sections involves division by a function of t only, our conclusions about the s and M_x^2 dependence of the differential cross-sections and about the validity of the FMSR are immune to uncertainties in the extraction procedure.

I. Factorization and Extraction of $pp \rightarrow Xp$ Cross-Sections -

The $pd \rightarrow Xd$ measurement was performed at Fermilab using an internal deuterium gas jet target. Elastic pd scattering was also studied[5] in the same p_{lab} and t-range. The elastic cross-section factorizes approximately like $(d\sigma/dt)^{pd} \simeq (d\sigma/dt)^{pp} \cdot F_d(p_{lab},t)$, where $F_d(p_{lab},t)$ is the coherence factor defined as

$$F_d(p_{lab},t) = \left[\frac{\sigma_\tau^{pd}}{\sigma_\tau^{pp}} (p_{lab}) \right]^2 \cdot |S(t)|^2 \tag{2}$$

Here, $\sigma_\tau^{pd(pp)}$ is the pd(pp) total cross-section and $S(t)$ is the deuteron form factor. In this region of small $|t|$, the data are described well by

$$|S(t)|^2 = e^{b_o t + ct^2} \tag{3}$$

with [5] $b_o = 26.4 \pm 0.2\ (\mathrm{GeV/c})^{-2}$ and $c = 62.3 \pm 1.1\ (\mathrm{GeV/c})^{-4}$. Over the p_{lab} range of the pd experiment, the factor $(\sigma_\tau^{pd}/\sigma_\tau^{pp})^2$ is approximately constant and has the value[6] of 3.6 to within better than 2% accuracy. Thus, the coherence factor takes the form

$$F_d(t) \equiv F_d\ (50 < p_{lab} < 400,\ |t| < 0.12) \simeq 3.6\ e^{26.4\ t\ +\ 62.3\ t^2} \tag{4}$$

Assuming that the inelastic cross-section factorizes in the same way as the elastic,

$$\frac{d^2\sigma}{dtdM_x^{\ 2}}\ (pd \to Xd) = \left[\frac{d^2\sigma}{dtdM_x^{\ 2}}\ (pp \to Xp)\right] \cdot F_d(t) \tag{5}$$

one may then obtain cross-sections for the reaction

$$p + p \to X + p \tag{6}$$

by dividing the measured cross-sections for $pd \to Xd$ by the elastic coherence factor. If the Glauber-type corrections for inelastic scattering are comparable to the corrections for elastic scattering ($\lesssim$ 10%), this procedure is expected to yield the correct cross-sections for $pp \to Xp$, including the values of the slope parameter, to within better than ~10%.

Factorization was successfully tested[1] in the $M_x^{\ 2} < 4\ \mathrm{GeV}^2$ region for $|t| = 0.025\ (\mathrm{GeV/c})^2$ and $p_{lab} = 180$ and 275 GeV/c (see Fig. 1). In Fig. 2,

we compare our extracted $pp \to Xp$ cross-sections for $p_{lab} = 275$ GeV/c and $|t| = 0.025$ $(GeV/c)^2$ with data from Fermilab[7,8] and ISR[9], where the points of references 8 and 9 have been obtained from the measured cross-sections at $|t| = 0.15$ and 0.16, respectively, by extrapolation using a slope of 6 $(GeV/c)^{-2}$. The agreement at low as well as high values of M_x^2 is good within the experimental error of ~10%. The peaking of the cross-section at low M_x^2/s is striking and the $1/M_x^2$ behavior in the region 5 $GeV^2 \lesssim M_x^2 \lesssim 0.05$ s is apparent.

II. M_x^2, t, and s Dependence of Extracted $pp \to Xp$ Cross-Sections -

In the resonance region, $M_x^2 < 5$ GeV^2, the M_x^2 distributions of the extracted pp cross-sections exhibit structure[1], with a prominent broad enhancement centered at $M_x^2 \simeq 1.9$ GeV^2 and a smaller peak at $M_x^2 \simeq 2.8$ GeV^2 probably to be identified with the $N^*(1688)$ state (see Fig. 3). A still smaller bump may be present at $M_x^2 \simeq 3.7$ GeV^2. For $M_x^2 > 5$ GeV^2, the cross-sections at fixed s behave[2] as $1/M_x^2$. The t-distributions for fixed M_x^2 are exponential[1,2] (see Fig. 4) with no sign of a turnover down to values of $|t| \simeq 0.03$ $(GeV/c)^2$. The slope parameter, $b(M_x^2)$, seems to be a function only of M_x^2, independent of p_{lab}. In the resonance region, $b(M_x^2)$ falls very rapidly from the value of ~20 $(GeV/c)^{-2}$ at $M_x^2 \sim 1.9$ GeV^2 to the average value[2] of 6.5 ± 0.3 $(GeV/c)^{-2}$ for $M_x^2 \gtrsim 5$ GeV^2.

Fig. 5a shows $b(M_x^2)$ versus M_x^2 for $p_{lab} = 275$ GeV/c. Fig. 5b shows the differential cross-section at $t = 0$ multiplied by M_x^2, obtained by extrapolating the data at higher $|t|$-values (Fig. 3) using the slopes in Fig. 5a. The M_x^2 distributions of $b(M_x^2)$ and of $M_x^2(d^2\sigma/dtdM_x^2)_{t=0}$ have a very similar shape. Dividing the values of $M_x^2(d\sigma/dtdM_x^2)_{t=0}$ in Fig. 5b by the values of the slopes

in Fig. 5a yields M_x^2 times the integral over t of the differential cross-section, $M_x^2(d\sigma/dM_x^2)$, shown in Fig. 5c. Within the errors, $M_x^2(d\sigma/dM_x^2)$ is constant all the way down to $M_x^2 \sim 1.7$ GeV^2, where it starts dropping towards the pion threshold at $M_x^2 \simeq 1.15$ GeV^2. Thus, the prominent low-mass enhancement at $M_x^2 \sim 1.9$ GeV^2 observed at small fixed t-values appears to be a manifestation of the increased value of the slope parameter. The cross-section for the production of a mass, $d\sigma/dM_x^2$, follows the simple $1/M_x^2$ behavior for all masses within the range of the pd experiment including the resonance region.

Our extracted $pp \to Xp$ cross-sections show a non-negligible energy dependence. An adequate fit of the differential cross-section in the TR region is given by[2]

$$\frac{d^2\sigma}{dtdM_x^2} = \frac{A(1 + B/p_{lab})}{M_x^2} b_o e^{b_o t} \tag{7}$$

where $A = 0.54 \pm 0.04$ mb, $B = 54 \pm 16$ GeV/c, and $b_o = 6.5 \pm 0.3$ (GeV/c)$^{-2}$. It is remarkable that this formula also describes well the average behavior of the cross-section in the resonance region provided b_o is replaced by $b(M_x^2)$ of Fig. 5a.

A pure triple-Pomeron (TP) coupling would require[3] (for our small values of $|t|$)

$$\frac{d^2\sigma}{dtd\nu} \simeq G_{PPP}(t)/\nu \tag{8}$$

where $\nu = M_x^2 - m_p^2 - t$ is the crossing symmetric variable and $G_{PPP}(t)$ is the TP coupling constant. At each given value of p_{lab}, our fitted result (7)

is compatible with a pure TP coupling. For $p_{lab} = 275$ GeV/c, a fit of our data for $M_x^2 > 5$ GeV^2 with equation (8) yields

$$G_{PPP}(t)\Big|_{p_{lab} = 275} = (3.87\pm0.29)\ e^{(6.5\pm0.3)t}\ \text{mb}\cdot(\text{GeV/c})^{-2} \qquad (9)$$

with a χ^2 of about 1 per degree of freedom. Below, we will use form (8) for our test of the FMSR. Here, we wish to emphasize that although at a fixed energy the data can be fitted by a simple TP coupling, the energy dependence as expressed in equation (7) is not expected from a pure TP coupling.

III. Test of the FMSR -

The first-moment finite mass sum rule states that[4] at fixed t

$$|t|\ \frac{d\sigma_{el}}{dt} + \int_0^N \nu\ \frac{d^2\sigma}{dtd\nu}\ d\nu = \int_0^N \nu \left[\frac{d^2\sigma}{dtd\nu}\right]_{TR} d\nu \qquad (10)$$

where $d\sigma_{el}/dt$ is the differential elastic scattering cross-section, $[d^2\sigma/dtd\nu]_{TR}$ is the fit to the inelastic cross-section in the TR region smoothly extrapolated to $\nu = 0$, and N is any ν corresponding to an M_x^2 lying between resonances. For fixed t, $d\nu = dM_x^2$. Figure 6 shows (i) the values of $\nu d^2\sigma/dtdM_x^2$ versus M_x^2 derived from our data at 275 GeV/c and $|t| = 0.035$ (GeV/c)^2 , (ii) the experimental value of $|t|d\sigma_{el}/dt$ which is represented as a Gaussian shaped area for illustrative purposes, and (iii) the fit to our data in the TR region of $\nu[d^2\sigma/dtdM_x^2]_{TR}$ extrapolated to $M_x^2 = m_p^2$, represented by the solid curve at the constant value of

3.1 mb·$(GeV/c)^{-2}$. Figure 6 illustrates that the sum of the areas under (i) and (ii) equals that of (iii) within a few percent. Thus we conclude that the data is in excellent agreement with the first-moment FMSR. The validity of this rule for other t-values within the range of the $pd \to Xd$ experiment is equally good.

We wish to thank Dr. Vladimir Rittenberg for many useful discussions.

This report is based on the work[1,2,5,7] of the USA-USSR Collaboration at the Internal Gas Jet Target of Fermilab. The members of the present collaboration are: Y. Akimov, L. Golovanov, S. Mukhin, G. Takhtamyshev, and V. Tsarev, Joint Institute for Nuclear Research, Dubna, U.S.S.R.; E. Malamud, R. Yamada, and P. Zimmerman, Fermi National Accelerator Laboratory, Batavia, Illinois; R. Cool, K. Goulianos, and H. Sticker, Rockefeller University, New York, New York; and D. Gross, A. Melissinos, D. Nitz, and S. Olsen, University of Rochester, Rochester, New York.

REFERENCES

1. Y. Akimov et al., Phys. Rev. Letters (to be published)
2. Y. Akimov et al., Phys. Rev. Letters (to be published)
3. See for example D.P. Roy and R.G. Roberts, Nucl. Physics B77, 240 (1974) and references therein.
4. A.I. Sanda, Phys. Rev. D6, 280 (1972); M.B. Einhorn, J. Ellis, and J. Finkelstein, Phys. Rev. D5, 2063 (1972).
5. Y. Akimov et al., "Proton-deuteron Elastic Scattering at Small Momentum Transfer from 50 to 400 GeV/c," submitted for publication to Phys. Rev.
6. A.S. Carroll et al., (to be published in Phys. Letters).
7. V. Bartenev et al., Phys. Letters 51B, 299 (1974).
8. K. Abe et al., Phys. Rev. Letters 31, 1527 (1973).
9. M.G. Albrow et al., Nucl. Phys. B72, 376 (1974).

FIGURE CAPTIONS

Figure 1 - Factorization test: Comparison of $(pd \to Xd)/F_d$ with $pp \to Xp$.

a) 180 GeV/c extracted pp data vs. 175 GeV/c pp data from ref. 7.

b) 275 GeV/c extracted pp data vs. 260 GeV/c pp data from ref. 7.

Figure 2 - Differential cross-sections for $pp \to Xp$ vs. M_x^2 for $s \sim 500$ GeV^2 and $|t| = 0.025$ (GeV/c)^2, obtained from the listed $|t|$-values using slopes given in the references. For the extrapolation of the CHLM and Rutgers — Imperial College data a slope of 6 (GeV/c)$^{-2}$ was used.

Figure 3 - Differential cross-sections vs. M_x^2 for $pp \to Xp$, extracted from $pd \to Xd$ at 275 GeV/c, for $|t| = 0.035$ (GeV/c)^2.

Figure 4 - Differential cross-sections vs. t for $pp \to Xp$, extracted from $pd \to Xd$, at $p_{lab} = 275$ GeV/c, for $M_x^2 = 1.9$, 2.7, 3.1, and 11 GeV^2.

Figure 5 - Values for $pp \to Xp$ vs. M_x^2, extracted from $pd \to Xd$ at 275 GeV/c.

a) The slope parameter, $b\ (M_x^2)$.

b) $d^2\sigma/dtdM_x^2$ multiplied by M_x^2 and extrapolated to $t = 0$ using $b\ (M_x^2)$.

c) Values of (b) above, divided by values of (a): $M_x^2\ (d\sigma/dM_x^2)$.

Figure 6 - Test of the first-moment FMSR: Values of $\nu(d^2\sigma/dtdM_x^2)$ vs. M_x^2 for $p_{lab} = 275$ GeV/c and $|t| = 0.035$ (GeV/c)^2.

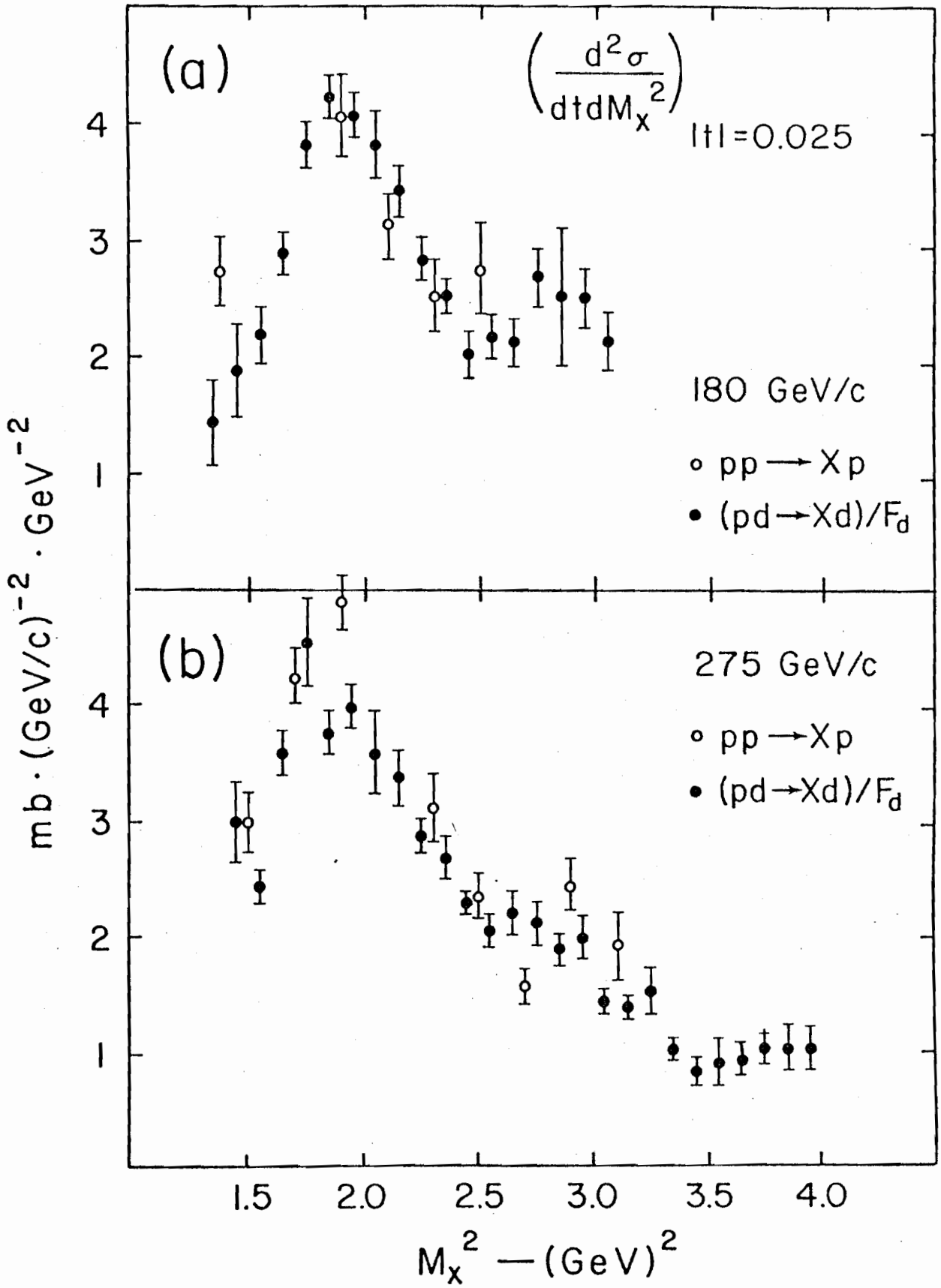
(a)
$\left(\frac{d^2\sigma}{dt dM_x^2}\right)$
|t|=0.025
180 GeV/c
○ pp → Xp
● (pd→Xd)/F_d
(b)
275 GeV/c
○ pp → Xp
● (pd→Xd)/F_d
mb · (GeV/c)^-2 · GeV^-2
1
2
3
4
1.5
2.0
2.5
3.0
3.5
4.0
M_x^2 — (GeV)^2

Fig. 1

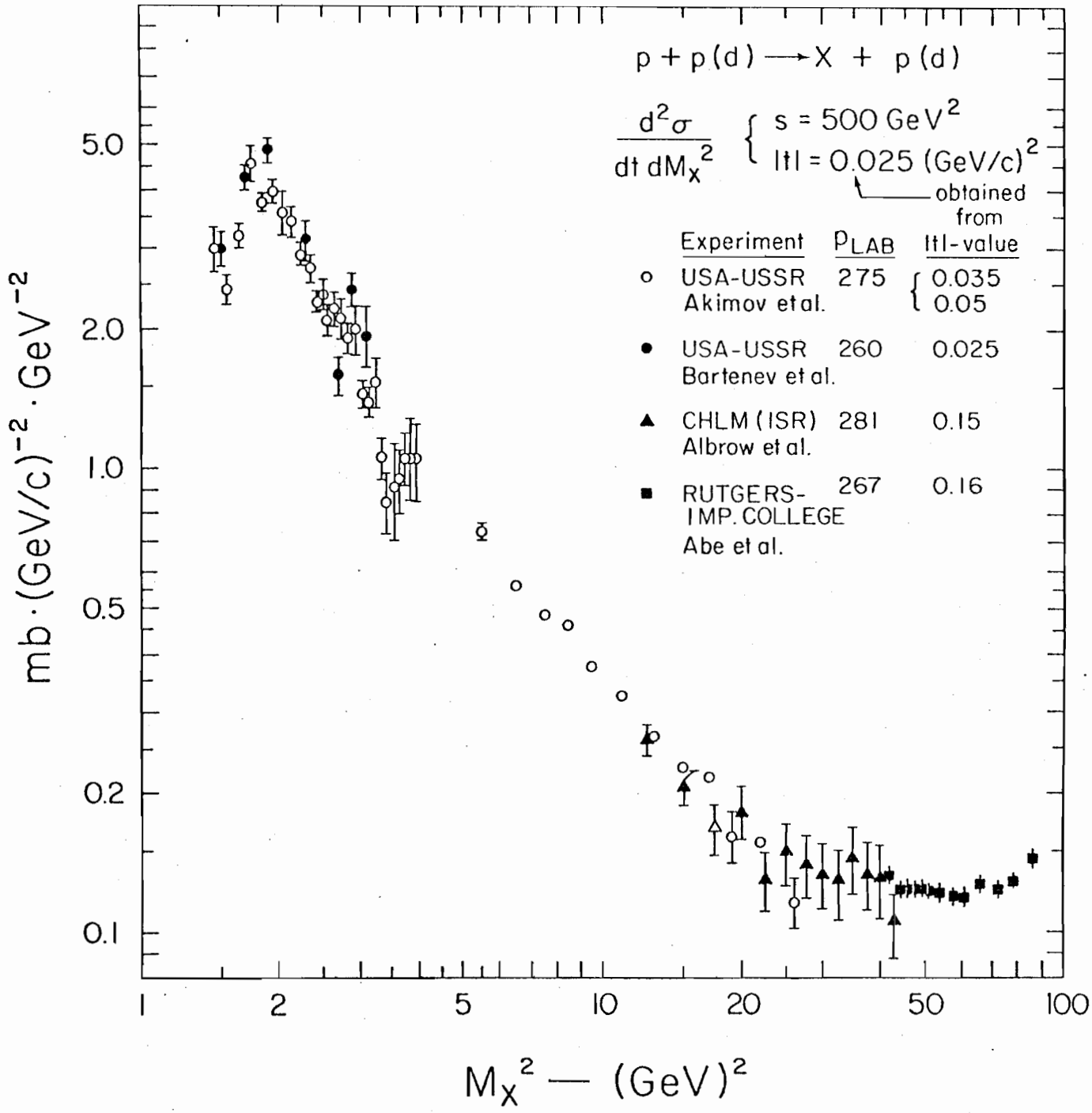
p + p(d) → X + p(d)
d²σ / dt dM_X²
s = 500 GeV²
|t| = 0.025 (GeV/c)²
obtained from |t|-value
Experiment
P_LAB
|t|-value
USA-USSR Akimov et al. 275 0.035 0.05
USA-USSR Bartenev et al. 260 0.025
CHLM (ISR) Albrow et al. 281 0.15
RUTGERS-IMP. COLLEGE Abe et al. 267 0.16
mb·(GeV/c)⁻²·GeV⁻²
5.0
2.0
1.0
0.5
0.2
0.1
1
2
5
10
20
50
100
M_X² — (GeV)²

Fig. 2

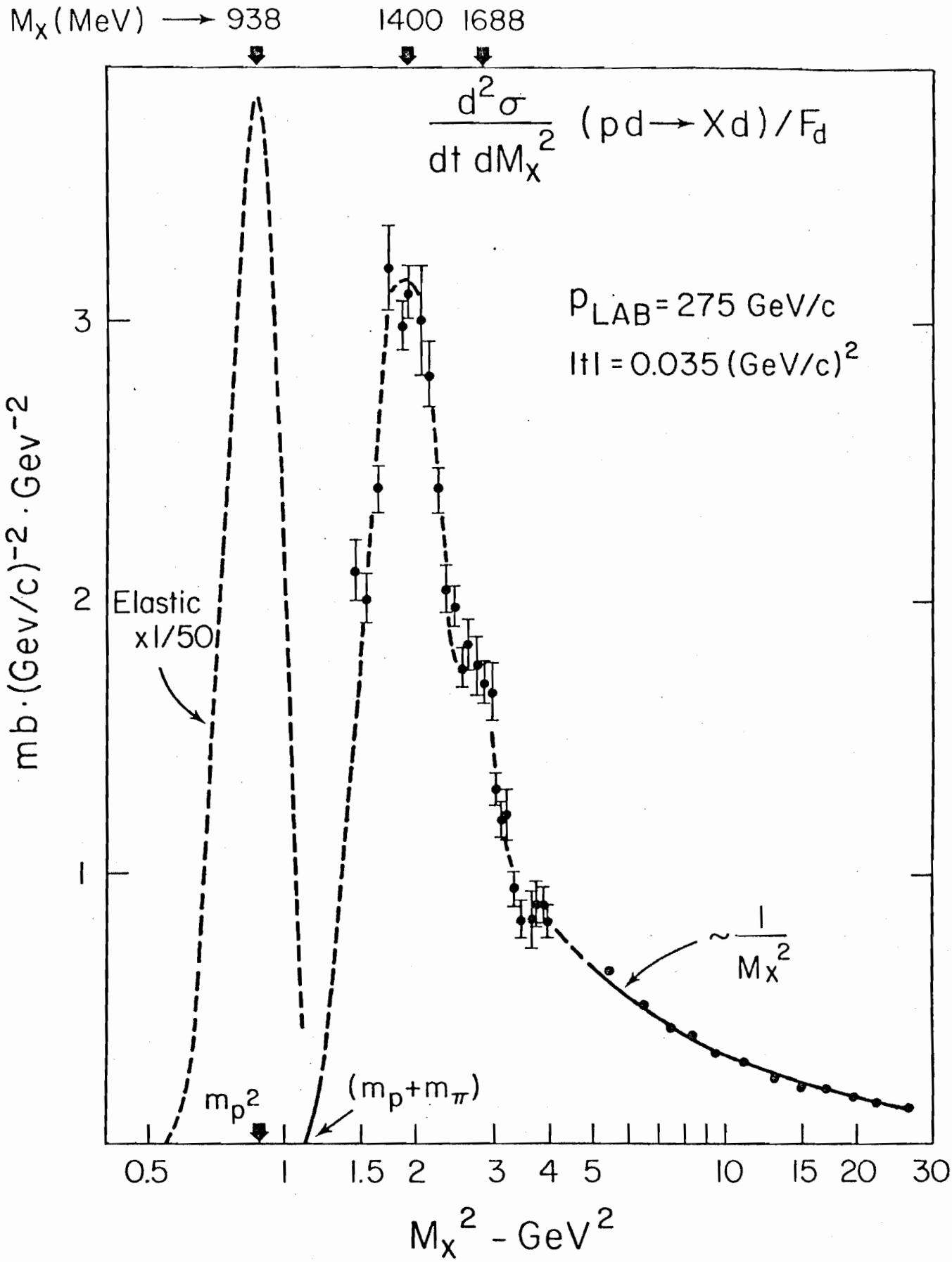
M_X (MeV) → 938
1400
1688
$\frac{d^2\sigma}{dt\, dM_X^2}$ (pd → Xd)/F_d
p_{LAB} = 275 GeV/c
|t| = 0.035 (GeV/c)^2
Elastic
x1/50
$\sim \frac{1}{M_X^2}$
m_p^2
$(m_p + m_\pi)$
mb·(Gev/c)$^{-2}$·Gev^{-2}
3
2
1
0.5
1
1.5
2
3
4
5
10
15
20
30
M_X^2 - GeV^2

Fig. 3

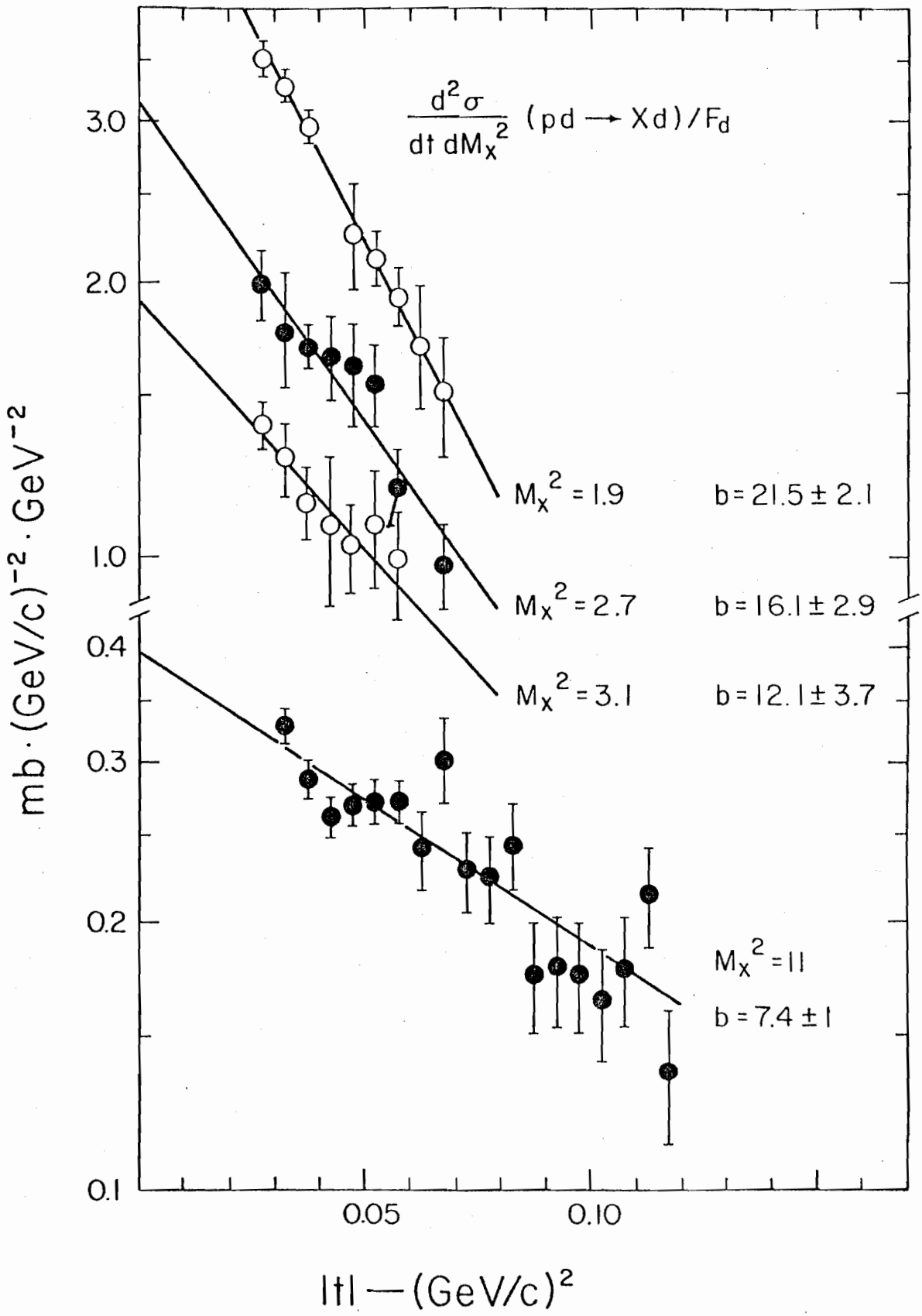
$\frac{d^2\sigma}{dt\,dM_X^2}$ (pd → Xd)/F_d
3.0
2.0
1.0
0.4
0.3
0.2
0.1
mb·(GeV/c)$^{-2}$·GeV^{-2}
M_X^2 = 1.9
b = 21.5 ± 2.1
M_X^2 = 2.7
b = 16.1 ± 2.9
M_X^2 = 3.1
b = 12.1 ± 3.7
M_X^2 = 11
b = 7.4 ± 1
0.05
0.10
|t| — (GeV/c)^2

Fig. 4

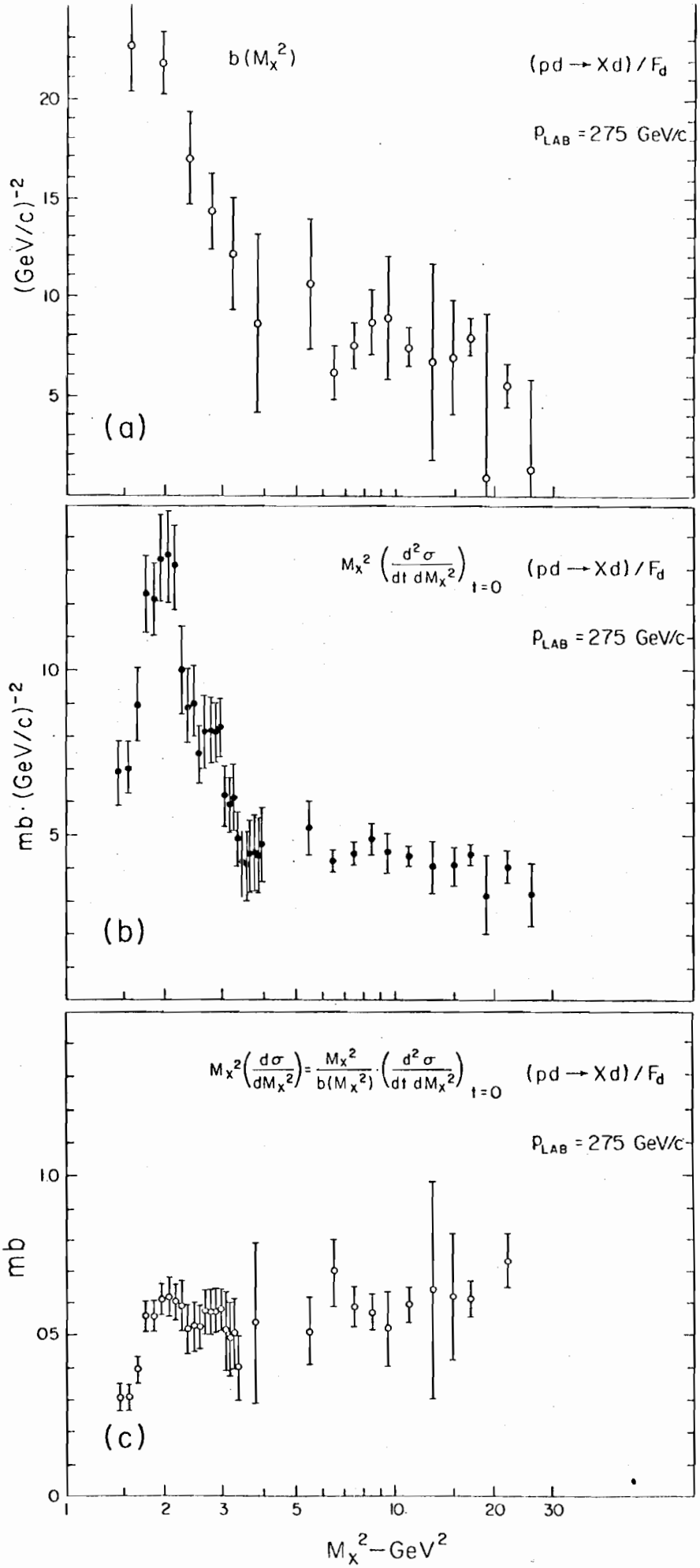
b(M_x^2)
(pd → Xd) / F_d
P_LAB = 275 GeV/c
(GeV/c)^-2
(a)
M_x^2 (d^2σ / dt dM_x^2)_t=0
(pd → Xd) / F_d
P_LAB = 275 GeV/c
mb · (GeV/c)^-2
(b)
M_x^2 (dσ / dM_x^2) = M_x^2 / b(M_x^2) · (d^2σ / dt dM_x^2)_t=0
(pd → Xd) / F_d
P_LAB = 275 GeV/c
mb
(c)
M_x^2 — GeV^2

Fig. 5

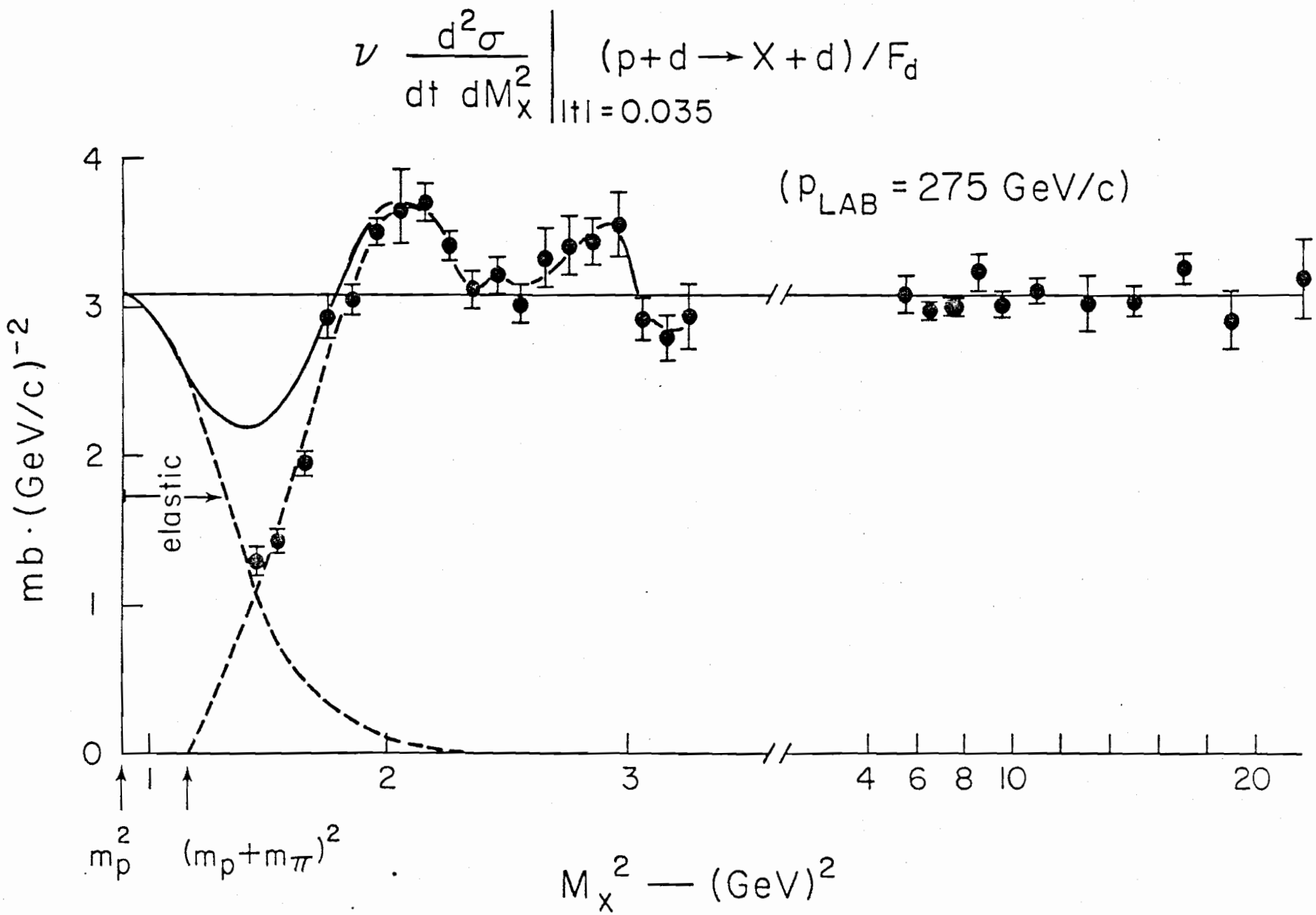
$\nu \frac{d^2\sigma}{dt\, dM_x^2}\Big|_{|t|=0.035} (p+d \rightarrow X+d)/F_d$
(p_{LAB} = 275 GeV/c)
mb · (GeV/c)$^{-2}$
elastic
0
1
2
3
4
1
2
3
4
6
8
10
20
m_p^2
$(m_p+m_\pi)^2$
M_x^2 — (GeV)^2

Fig. 6